

Bilateral Contract for Load Frequency and Renewable Energy Sources Using Advanced Controller

Krishan Arora¹, Gyanendra Prasad Joshi², Mahmoud Ragab^{3,4,5,*}, Muhyaddin Rawa^{6,7,8}, Ahmad H. Milyani^{6,7}, Romany F. Mansour⁹ and Eunmok Yang¹⁰

¹School of Electronics and Electrical Engineering, Lovely Professional University, Phagwara, 144001, Punjab, India

²School of Department of Computer Science and Engineering, Sejong University, Seoul, 05006, Korea

³Information Technology Department, Faculty of Computing and Information Technology, King Abdulaziz University, Jeddah, 21589, Saudi Arabia

⁴Centre for Artificial Intelligence in Precision Medicines, King Abdulaziz University, Jeddah, 21589, Saudi Arabia

⁵Mathematics Department, Faculty of Science, Al-Azhar University, Naser City, 11884, Cairo, Egypt

⁶Center of Research Excellence in Renewable Energy and Power Systems, King Abdulaziz University, Jeddah, 21589, Saudi Arabia

⁷Department of Electrical and Computer Engineering, Faculty of Engineering, King Abdulaziz University, Jeddah, 21589, Saudi Arabia

⁸King Abdullah City for Atomic and Renewable Energy (K. A. CARE), Riyadh, Saudi Arabia

⁹Department of Mathematics, Faculty of Science, New Valley University, El-Kharga, 72511, Egypt

¹⁰Department of Information Security, Cryptology, and Mathematics, Kookmin University, Seoul, 02707, Korea

*Corresponding Author: Mahmoud Ragab. Email: mragab@kau.edu.sa

Received: 08 January 2022; Accepted: 27 April 2022

Abstract: Reestablishment in power system brings in significant transformation in the power sector by extinguishing the possession of sound consolidated assistance. However, the collaboration of various manufacturing agencies, autonomous power manufacturers, and buyers have created complex installation processes. The regular active load and inefficiency of best measures among varied associates is a huge hazard. Any sudden load deviation will give rise to immediate amendment in frequency and tie-line power errors. It is essential to deal with every zone's frequency and tie-line power within permitted confines followed by fluctuations within the load. Therefore, it can be proficient by implementing Load Frequency Control under the Bilateral case, stabilizing the power and frequency distinction within the interrelated power grid. Balancing the net deviation in multiple areas is possible by minimizing the unbalance of Bilateral Contracts with the help of proportional integral and advanced controllers like Harris Hawks Optimizer. We proposed the advanced controller Harris Hawk optimizer-based model and validated it on a test bench. The experiment results show that the delay time is 0.0029 s and the settling time of 20.86 s only. This model can also be leveraged to examine the decision boundaries of the Bilateral case.

Keywords: Bilateral contract; load frequency control; optimization; harris hawks optimizer



This work is licensed under a Creative Commons Attribution 4.0 International License, which permits unrestricted use, distribution, and reproduction in any medium, provided the original work is properly cited.

1 Introduction

Load Frequency Control (LFC) issue is extremely critical and novel arena of investigation in interrelated power systems in the power system process. The generators functions in the service zone and steadily swung the speed to correspond the power angles and frequency to the precise quantity of fixed and enthusiastic circumstances. It is obligatory to accomplish the frequency at definite and adequate restrictions, but nonstop dissimilarity in load cannot be overlooked due to its unstable nature. An ethical load frequency control system has the ability to equilibrium the tie-line power and system frequency within their limits [1]. This paper presents advanced controllers like Binary moth Flame optimizers and Harris Hawks Optimizers to study the multi-area load frequency control (LFC) problem along with renewable energy sources compared to conventional proportional-integral (PI) controllers. There are some significant contributions due to which these advanced controllers are like:

- i) Unlike conventional PI controllers, it maintains the system frequency without any steady-state error.
- ii) Instantaneously reduces the settling time and responds to the peak overshoot within a short time than the conventional PI controller.
- iii) Instantly responds to the different load disturbances and makes the system stable within a short time.

Our contributions in this work are as follows: first, we propose the two variants of binary MFO to solve the frequency constraint issues. We implemented two different binary variants for improving the performance of Moth Flame Optimizer (MFO) for discrete optimization problems. In the first variant, i.e., Binary Moth Flame Optimizer (BMFO1), the coin flipping-based selection probability of binary numbers is used. We used the improved Sigmoid Transformation in the second variant called BMFO2. These binary MFO algorithms along with Harris Hawks Optimizer (HHO) algorithms, are tested and analyzed under Bilateral contract. The following section of this paper is as described: Section 1 introduces the Load Frequency Control problem concept. Section 2 presents a transfer function model of Hydro-Thermal and Solar-Thermal power plants. Sections 3 and 4 introduce the concept of conventional PI as well as advanced controllers in which a novel approach named HHO is defined. In Sections 5 and 6, Bilateral Contract and its PI gain values are explained. Section 7 concludes results and discussions for both conventional controllers as well as for Advanced Controllers. Finally, the conclusion and future scope are presented in Section 8.

2 Multi-Area Hydro-Thermal and Solar-Thermal Transfer Function

A multi-area interconnected power structure with thermal, hydro, and solar-thermal systems [2,3] is considered in this work. There is a growing attentiveness in the influence of Non-conventional energy sources on power scheme operation and control, as the application of this source is expanding world-widely. Non-conventional energy technologies are one of the finest expertise for generating cheaper electrical energy, hygienic environment and are almost available during the year. Solar energy is the most promising source for the generation of electric power throughout the world. Compared to wind energy systems, solar energy systems have much more applications like Solar cooking systems, Solar water heaters, and solar photovoltaic systems. In India, the solar power systems and various solar energy applications were utilized in private sectors, which are higher than in Government sectors. Similarly, more installations of wind energy generations are with private sectors rather than government sectors. In the future, these non-conventional energy sources will be the major sources of power generation [4].

2.1 Thermal Power System

In the Thermal generating unit, as explained, the generator of the turbine work like a prime mover in which it receives the mechanical energy from the boiler via steam. This steam turbine is meticulous by a speed governor. With a small increment in demand, the unbalance among the production of electricity and requirement is indirectly detected by the governor with respect to fluctuation in frequency [5]. Dependent on the value of detected frequency, the speed governor using hydraulic amplifiers modifies the valve location of steam, which regulates the frequency.

Transfer Function Model of Thermal Power System

The mechanisms of the thermal power scheme, i.e., speed regulator, steam turbine, hydraulic amplifier, and power system, are modeled as single order time constant for doing small-signal analysis. The disconcerted exact model of the thermal generating unit with the primary controller of speed governor is exposed in Fig. 1. It comprises of a non-reheat steam turbine as a prime mover, which drives a generator to supply energy to the power system.

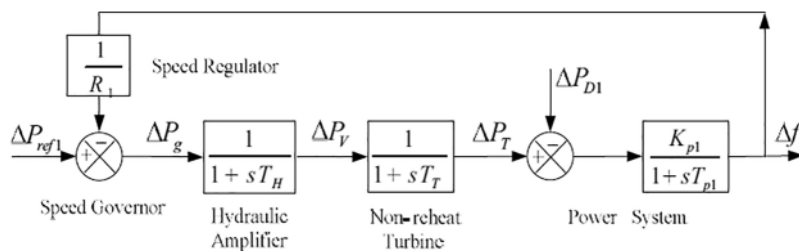


Figure 1: Transfer function representation of thermal power system

The inputs to speed governor are reference power settings (ΔP_{ref1}) and fluctuation in frequency (Δf_i). The production of speed governor regulates the input steam of the turbine as per the demand requirement.

The transfer function of speed governor is assumed in Eq. (1) as;

$$\Delta P_g = \Delta P_{ref1} - \left(\frac{1}{R_1}\right) \Delta f_i \tag{1}$$

The speed governor fails to operate against high-pressure steam. Therefore, by using numerous phases of a hydraulic amplifier, large mechanical forces position the gate valves of the turbine against high-pressure steam. The transfer function of the hydraulic amplifier is expressed in Eq. (2) as:

$$\Delta P_v = \left(\frac{1}{1 + sT_H}\right) \Delta P_g \tag{2}$$

In this research, a non-reheat turbine is used as the prime mover. The equation that explains turbine operation is furnished in Eq. (3) as:

$$\Delta P_T = \left(\frac{1}{1 + sT_T}\right) \Delta P_v \tag{3}$$

The output power of the turbine, energies the generator to deliver the electric power. The transfer function of power arrangement contains generator with load disorder is expressed in Eq. (4) as:

$$\Delta P_T - \Delta P_{D1} = \left(\frac{K_{p1}}{1 + sT_{p1}}\right) \Delta f_i \tag{4}$$

2.2 Hydro Power System

The features of Hydro turbines are not similar to Thermal turbines. In Hydro plants, water acts as a origin for generating mechanical energy to energies the turbine. Because it takes slight time to ignite but more time interval to interact during the regular process due to the tremendous inertia of water. The unbalance amongst generation and consumption is detected indirectly with respect to fluctuation in oscillations by the regulator, which regulates the inlet of water to turbine [6].

Transfer Function Representation of Hydro Power System

The statistical model of the arrangement with speed regulator, hydro turbine, and power system is published as a report, and the transfer function representation of Hydro generating unit with speed regulator as main LFC is revealed in Fig. 2.

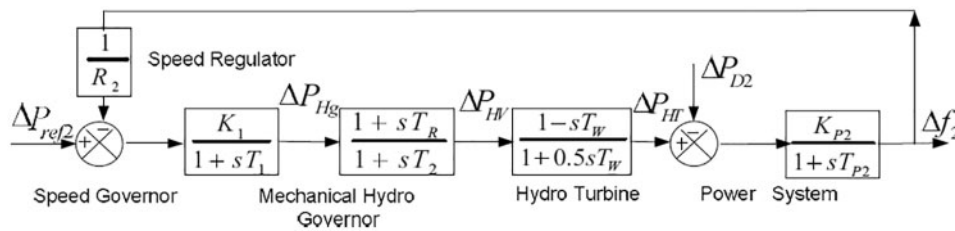


Figure 2: Transfer function model of the hydropower system

The operation of the speed regulator of the Hydro generating unit is like that of the steam-generating unit. In this paper, the low head hydro generating unit is measured for literature. Eq. (5) specifies the transfer role of the hydro governor as follows.

$$\Delta P_{HV} = \frac{1 + sT_R}{1 + sT_2} \Delta P_{Hg} \tag{5}$$

where $\Delta P_{Hg} = \frac{K_1}{1 + sT_1} (\Delta P_{ref/2} - \frac{1}{R_2} \Delta f_2)$

The reset time TR is specified in Eq. (6)

$$TR = [5.0 - (T_w - 1.0) 0.5] T_w \tag{6}$$

where, T_w is water time constant ranging from 1 to 4 s for low head Hydro turbines. $T1$ is transient droop time constant in second, which is shown in Eq. (7)

$$T1 = \frac{R_{TD}}{R_{PD}} T_R \tag{7}$$

where RTD is the temporary droop that is expressed in Eq. (8)

$$RTD = [2.3 - (TH - 1.0) 0.15] \frac{T_w}{T_M} \tag{8}$$

in which T_M is identical to 2H.

In the Hydro system, water acts as input power to run the turbine regulated by the hydro governor. The transfer purpose of the Hydro turbine is shown in Eq. (9)

$$\Delta P_{HT} = \frac{1 - sT_w}{1 + 0.5sT_w} \Delta P_{HV} \tag{9}$$

The transfer function of the generator is combined to power arrangement with the facility to provide load fluctuation comparable to the thermal power system as equipped in Eq. (4).

2.3 Solar-Thermal Power Plant

Non-conventional energy sources like Solar energy have huge energy potential. Photovoltaic (PV) system and Intense Solar Power (ISP) are the arrangements that can generate energy from solar energy. ISP is getting significance all over the world as its having an extensive area of the collector field. A comparative study of solar-thermal generating units with various collectors like flat plates and parabolic trough collectors has also been examined [7]. The rate of transform of output hotness is shown by the below Eq.

$$\frac{dT_o(t)}{dt} = \frac{A\eta_o}{C} I(t) - \frac{U_L A}{C} [T_a(t) - T_c(t)] + \frac{v(t)}{V} [T_i(t) - T_o(t)] \quad (10)$$

where,

$$T_a(t) = \frac{T_i(t) + T_c(t)}{2}$$

By assuming a constant rate of flow of working fluid, Eq. (10) becomes

$$\frac{dT_o(t)}{dt} + \left[\frac{U_L A}{2C} + \frac{u}{V} \right] T_o(t) = \frac{A\eta_o}{C} I(t) + \left[\frac{u}{V} - \frac{U_L A}{2C} \right] T_i(t) + \frac{U_L A}{C} T_c(t) \quad (11)$$

After Laplace Transformation, we get

$$\frac{A\eta_o}{C} I(s) + \left[\frac{u}{V} - \frac{U_L A}{2C} \right] T_i(s) + \frac{T_s}{T_s S + 1} \times \frac{U_L A}{C} T_c(s) \quad (12)$$

where T_s is the time constant of the solar collector and is given by Eq. (13)

$$T_s = 1 / \left(\frac{U_L A}{2C} + \frac{u}{V} \right) \quad (13)$$

The changes in the inlet and atmospheric temperature are minimal. Hence transfer purpose of solar irradiance is given by

$$G(s) = \frac{K_s}{1 + T_s S} \quad (14)$$

where K_s is the gain of the solar field.

2.4 Tie-Line

The transfer function of the Thermal and Hydro generating unit revealed in Figs. 1 and 2 are considered to be a control area assuming that the area contains either Hydro or Thermal power plant alone, and they are incoherent operation. All the generators, turbines, and speed governors in a control area have similar characteristics, and they are said to be operating incoherent.

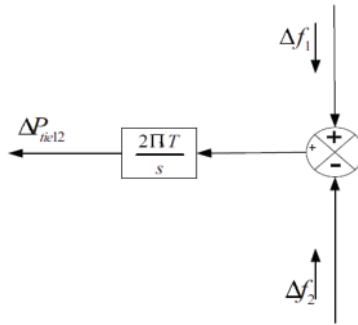
The power systems contain various control areas which are organized by tie-line to recover the dependability and constancy of the arrangement. When both areas are interrelated, the variation of load in any area will be remunerated by entire areas, but the net lively flow of power among the areas would not go beyond the boundaries [8].

Transfer Function Model of Tie-Line

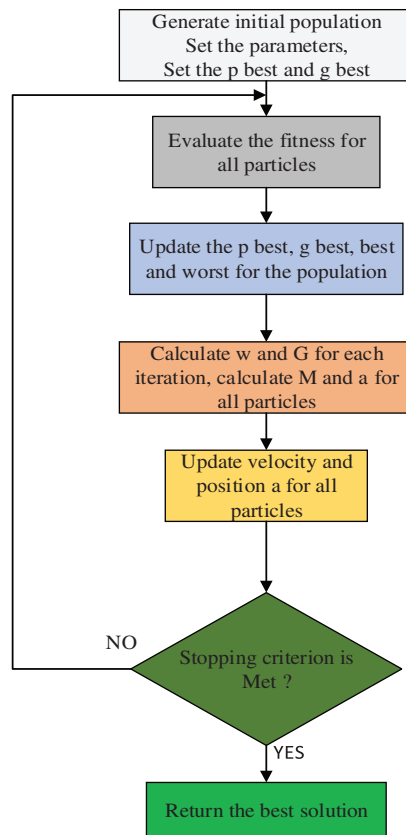
Tie-line is a medium that combines two areas. The flow of power through the line is based on the contract between the areas. The flow of power by transmission line is articulated in Eq. (15) as;

$$\Delta P_{tie12} = \frac{2\Pi T}{s} (\Delta f_1 - \Delta f_2) \quad (15)$$

The transfer function model of the tie-line is expressed in Eq. (15) is exposed in Fig. 3a.



(a) Transfer Function representation of Tie line



(b) Flowchart

Figure 3: (a) Transfer function representation of tie line. (b) Flowchart

3 Conventional Proportional Integral Controller

The proportional-integral (PI) controller is broadly used in industries, for many applications, because of its flexibility and simplicity. In a PI controller, proportional term increases the stability and produces a large-frequency reaction. The integral term makes steady-state inaccuracy to zero. Thus, the transient and steady states are improved by the PI controller. In this controller, merely two gains are required to be modified which leads to transient stability increase, and zero steady error. The main drawback of the controller is that it produces an overshoot in the output of the LFC system [9]. Nevertheless, the PID controller is not used in this work, even though the D controller diminishes the overshoot time with the I controller. It strengthens the distortion signal, and the system may become unstable.

Eq. (16) is the mathematical representation of the PI controller and the mathematical model of the PI controller, as shown in Fig. 4.

$$U(t) = K_p ACE_i + K_i \int_0^t ACE_i dt \tag{16}$$

where the gain of the P controller is represented with K_p , K_i is gain of the I controller, and U is PI controller control outcome. By comparing reference signal Y_r and the feedback signal y , the error signal e can be calculated from Area Control Error (ACE) as

$$e = ACE = y_r - y \tag{17}$$

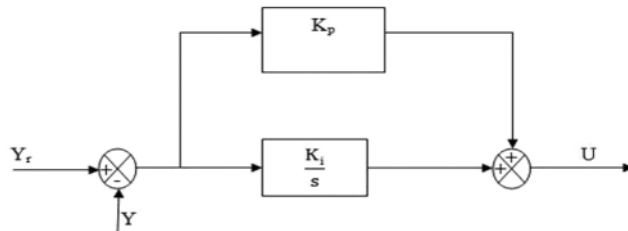


Figure 4: Representation of PI controller

On taking the Laplace transform of Eq. (17), the PI controller is obtained as shown in Eq. (18)

$$U(s) = K_p ACE_i(s) + \frac{K_i}{s} ACE_i(s) \tag{18}$$

$$U(s) = ACE_i(s) \left(K_p + \frac{K_i}{s} \right)$$

$$\frac{U(s)}{E(s)} = K_p \left(1 + \frac{K_i}{K_p s} \right)$$

$$\frac{U(s)}{E(s)} = K_p \left(1 + \frac{1}{T_i s} \right) \tag{19}$$

where $T_i = \frac{K_p}{K_i}$

$$G_{C(s)} = \frac{U(s)}{E(s)} = K_p \left(1 + \frac{1}{s T_i} \right) \tag{20}$$

From the PI controller, it is a lag compensator. It improves the steady-state characteristic of the arrangement. By connecting this type of controller, the compensated scheme urges by 1, making the structure unstable. Therefore, to get a stable structure, the values of K_p and T_i should be appropriately designed.

In a single area LFC scheme, the output parameter to be controlled is frequency deviation alone. However, in a two-area power scheme, every zone is interconnected with another area, using tie-line, and therefore both tie-line power and frequency need to be controlled. Control of the tie-line bias is a suitable strategy for scheming a conventional controller for a two-area LFC scheme.

Whenever frequency deviation occurs, it is the duty of PI controller to produce a control signal, with which the frequency deviation can be made to zero. Therefore, for the optimal operation of the LFC system, the gains of K_p and K_i need to be tuned. Many researchers developed different methods for tuning the gains of PI controllers have proposed different methods for modification of PI controllers [10].

4 Advanced Controllers

4.1 Binary Moth Flame Optimizer (BMFO1)

The basic MFO is a nature enthused heuristic explore a technique that imitates the navigation possession of moths about artificial lights. BMFO1 is a recently predictable meta-heuristics search algorithm suggested [11], which is re-energized by navigation actions of moth and their meeting close to the beam. It helps to recover the exploitation explore of moths and diminish the number of flames. Even if moths have a challenging potential to sustain a protected loom with respect to the moon and grip a bearable assembly for traveling in a traditional scratch for broad remoteness, they are also caring in a serious/inoperative bowed pathway over a replicated source of illumination.

4.2 Modified Sigmoid Transformation (BMFO2)

The binary calibration of stable quest accommodation and spaces of investigating council, resolution to binary searching domicile could be required to optimize binary ecological matter like LFC. A customized sigmoidal transfer function is assumed in the projected work, which has better presentation than any more substitute of it as depicted in. Basic Moth Flame Optimizer applied with modified sigmoidal transformation is used to bring the binary graph of authentic moth value and flame location for setting up LFC difficulty [12].

4.3 Harris Hawks Optimizer

HHO [13] is a gradient-free and population-focused algorithm containing unfair and investigative steps for wonder swoop, the fauna of assessment of prey, and assorted ploy built on brutal speculation of Harris hawks.

4.3.1 Bilateral Contract

The Bilateral Contract epitomizes the reciprocated, jointly argument of tapered power among Distribution Companies (DISCO) and Generation Companies(GENCO). As per this contract, GENCOs and DISCOs exchange power with respect to the prescribed contract to satisfy load requirements for a consistent energy structure process. The Distribution Participation Matrix signifies a bilateral contract for DISCO and GENCO as revealed below [14, 15].

4.3.2 PI Gain Values for Bilateral Contract Case [16,17]

The Proportional and Integral Gain values for Load Frequency Control system under Bilateral Contract is as follows:

5 Results and Discussion

The LFC scheme delivers the consistent action of the power structure by constantly balancing the resource of electricity with the response, while also confirming the accessibility of adequate supply volume in upcoming periods. In this paper, binary variations of moth flame optimizer and HHO has been analyzed for Bilateral contracts. This investigates that proposed HHO approach suggestions are offering better results as associated with substituting labeled meta-heuristics search algorithms. In upcoming work, the effectiveness of the HHO technique is deliberate for the optimal response of various other industrial concerns.

5.1 Bilateral Case for Multi-Area Thermal Hydro System with Conventional PI Controller

Bilateral Case shows [18] in Fig. 4, whose gain values are given in Tab. 1 are obtained using MATLAB/Simulink. The developed system is endangered to unit period load disturbances of 0.01 p.u in Area 1 alone. The reaction of the arrangement is exposed in Figs. 5 to 7.

Table 1: PI gain values

PI controller gain	Bilateral case
KP1	0.4301
Ki1	-7.0200E-06
KP2	0.1852
Ki2	-0.7261

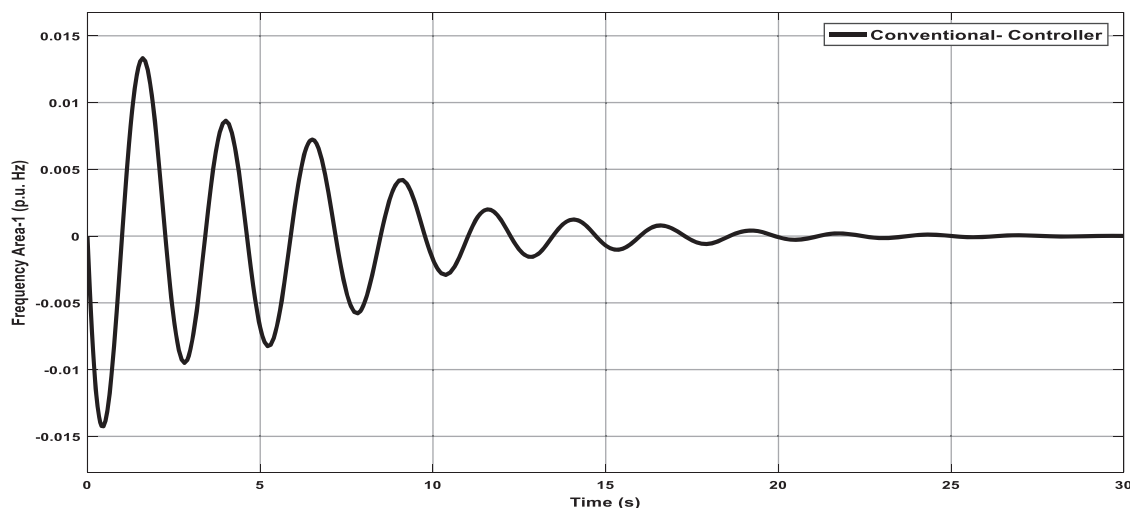


Figure 5: Response of bilateral case of hydro-thermal system for Area-1 tuned with conventional-controller

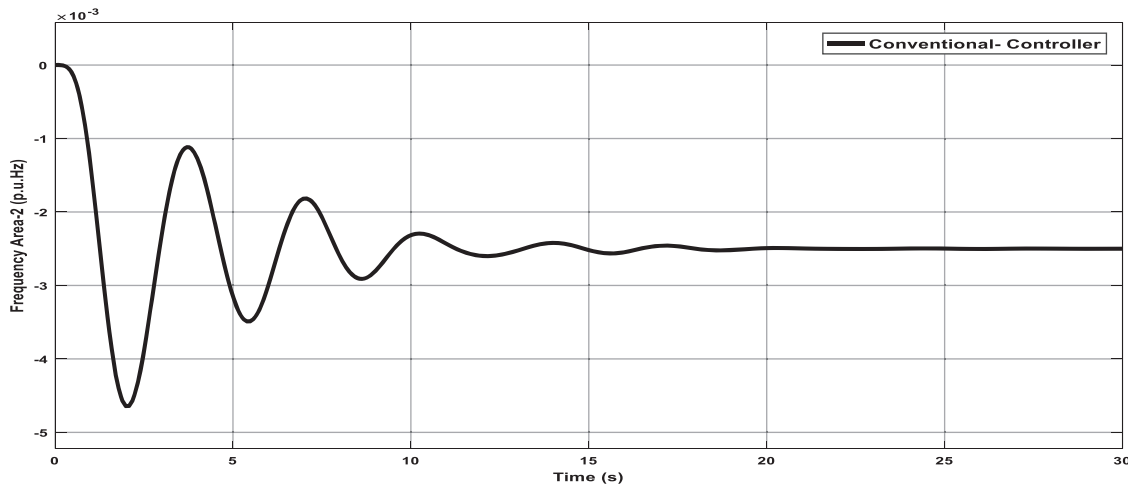


Figure 6: Response of bilateral case of hydro-thermal system for Area-2 tuned with conventional-controller

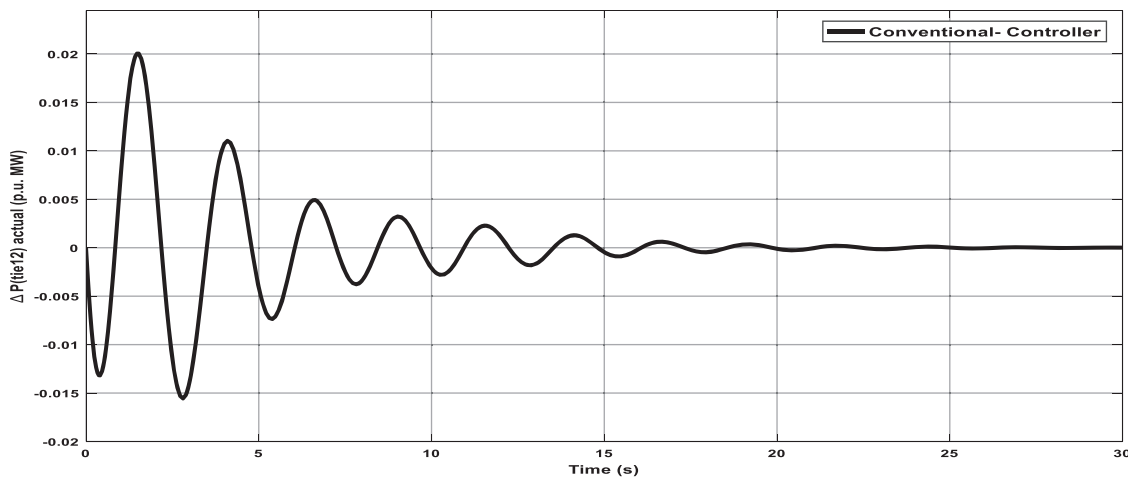


Figure 7: Response of bilateral case of hydro-thermal system for deviation in tie-line power tuned with conventional-controller

It is analyzed from Fig. 5 and Tab. 2 that the dynamic response of Hydro-Thermal system for Area-1 tuned with Conventional-Controller is plotted. The outcomes obtained show improved results with delay time = 0.01 s and settling time of 22 s.

It is analyzed from Fig. 6 and Tab. 3 that the dynamic response of Hydro-Thermal system for Area-2 tuned with Conventional-Controller is plotted. The outcomes obtained show improved results with delay time = 3.12 s and settling time of 22 s.

It is analyzed from Fig. 7 and Tab. 4 that the dynamic response of Hydro-Thermal system for deviation in tie-line control tuned with Conventional-Controller is plotted, and the outcomes obtained shows improved results with delay time = 0.85 s and settling time of 22 s.

Table 2: Graph analysis of Area-1 frequency with conventional-controller under bilateral contract

Parameters	Bilateral case
Delay time	0.01
Rise time	0.002
Peak overshoot time	0.017
Settling time	22

Table 3: Graph analysis of Area-2 frequency with conventional-controller under bilateral contract

Parameters	Bilateral case
Delay time	3.12
Rise time	1.15
Peak overshoot time	3.85
Settling time	22

Table 4: Graph analysis of divergence in tie-line control tuned with conventional-controller using bilateral contract

Parameters	Bilateral case
Delay time	0.85
Rise time	4.12
Peak overshoot time	5.84
Settling time	22

5.2 Bilateral Case for Multi-Area Thermal Hydro System with Integration of Solar-Thermal Power Plant Using Advance Controllers

The various dynamic responses with penetration of Solar in mutual areas and tie-line [19] as shown in Figs. 9.

It is analyzed from Tab. 5 that the dynamic response of Area-1 frequency with respect to time in seconds with various controllers like Conventional, PSO, MFO, BMFO1, BMFO2, and HHO under Bilateral Contract are compared. The comparative outcomes obtained show improved results of the HHO [20] controller with delay time = -0.835 s and settling time of 20.86 s.

It is analyzed from Fig. 8 and Tab. 6 that the dynamic response of Area-2 frequency with respect to time in seconds with various controllers like Conventional, PSO, MFO, BMFO1, BMFO2, and HHO under Bilateral Contract are compared. The comparative outcomes obtained show improved results of the HHO controller with delay time = 0.0023 s and settling time of 20.86 s.

It is analyzed from Fig. 9 and Tab. 7 that the active retort of Deviation in actual tie-line power flow with respect to time in seconds with various controllers like Conventional, PSO, MFO, BMFO1, BMFO2, and HHO under Bilateral Contract are compared. The comparative outcomes obtained show improved results of the HHO controller with delay time = 0.0029 s and settling time of 20.86 s.

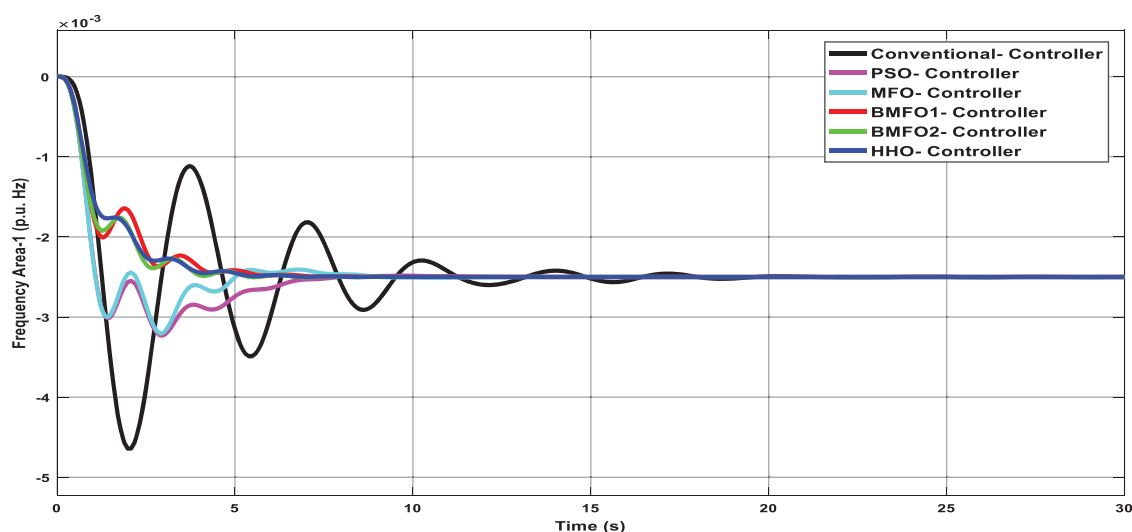


Figure 8: Dynamic rejoinder of Area-1 frequency with different controllers using bilateral contract

Table 5: Graph analysis of Area-1 frequency with a diverse controller using bilateral contract

Controller	Delay time	Rise time	Peak overshoot time	Settling time
Conventional	-2.414	-4.205	-4.668	23.39
PSO	-1.508	-2.715	-3.015	21.17
MFO	-1.503	-2.705	-3.005	21.01
BMFO1	-1.003	-1.805	-2.005	21.43
BMFO2	-0.978	-1.766	-1.955	21.43
HHO	-0.835	-1.499	-1.665	20.86

Table 6: Graph analysis of Area-2 frequency with different regulator using bilateral contract

Controller	Delay time	Rise time	Peak overshoot time	Settling time
Conventional	0.0066	0.0118	0.0131	23.39
PSO	0.0031	0.0047	0.0052	21.17
MFO	0.0045	0.0074	0.0082	21.01
BMFO1	0.0026	0.0046	0.0051	21.43
BMFO2	0.0027	0.0048	0.0053	21.43
HHO	0.0023	0.0041	0.0045	20.86

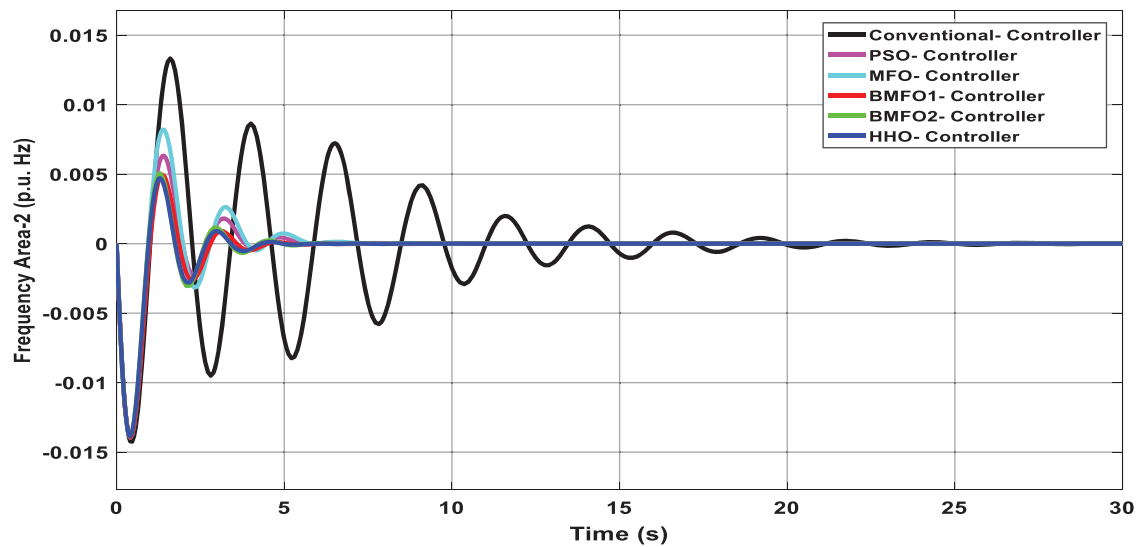


Figure 9: Dynamic reaction of Area-2 frequency with a different controller using bilateral case

Table 7: Graph analysis of divergence in actual tie-line power flow with a different controller using bilateral contract

Controller	Delay time	Rise time	Peak overshoot time	Settling time
Conventional	0.0106	0.0190	0.0211	23.39
PSO	0.0043	0.0077	0.0085	21.17
MFO	0.0063	0.0114	0.0125	21.01
BMFO1	0.0033	0.0059	0.0065	21.43
BMFO2	0.0031	0.0055	0.0061	21.43
HHO	0.0029	0.0053	0.0058	20.86

It is analyzed from [Figs. 10, 11](#) and [Tab. 8](#) that the dynamic response of Deviation in tie-line error with respect to time in seconds with various controllers like Conventional, PSO, MFO, BMFO1, BMFO2, and HHO under Bilateral Contract are compared. The comparative outcomes obtained show improved results of the HHO controller with delay time = 1.276 s and settling time of 19.8 s.

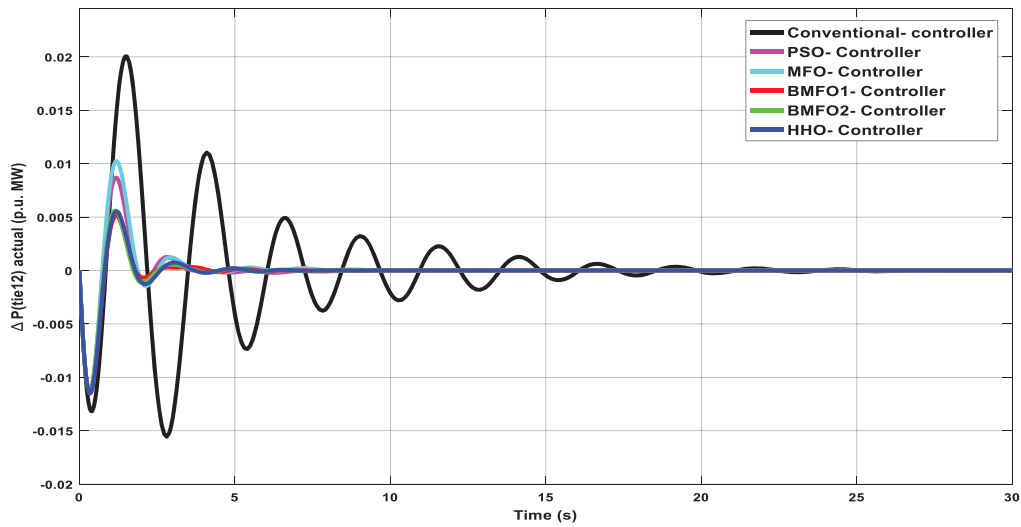


Figure 10: Digression in genuine tie-line power flow with a different controller using bilateral contract

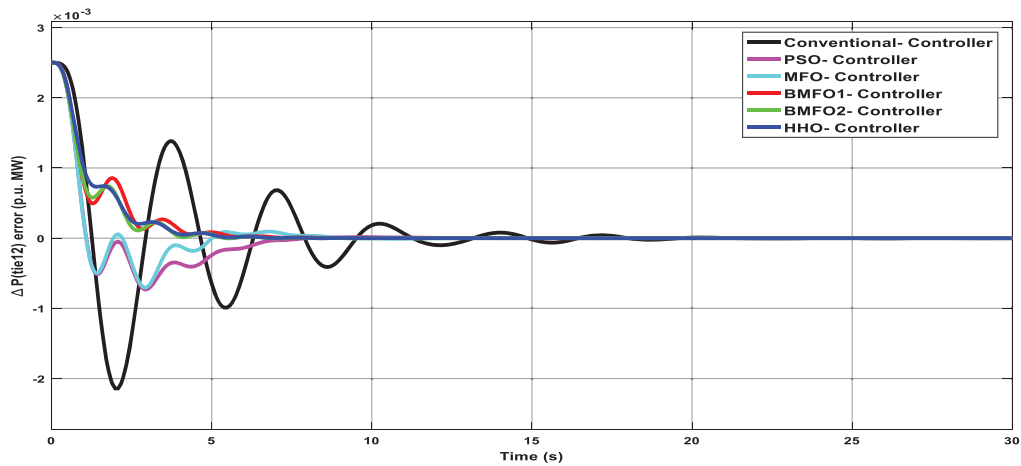


Figure 11: Divergence in tie-line fault with different controllers using bilateral contract

Table 8: Graph analysis of divergence in tie-line fault with diverse controllers using bilateral case

Controller	Delay time	Rise time	Peak overshoot time	Settling time
Conventional	1.284	2.311	2.568	22
PSO	1.278	2.299	2.555	21.430
MFO	1.277	2.298	2.554	21.3
BMFO1	1.277	2.297	2.553	21.02
BMFO2	1.277	2.296	2.552	20.1
HHO	1.276	2.295	2.551	19.8

6 Conclusion

Proportional Integral controllers are used in industries and also in power systems for many applications. The power system's consistent operation necessitates a constant balancing of source and load as per recognized operating criteria. The LFC structure offers the minute-to-minute unswerving operation of the power system by managing demand for power with supply with confirming the availability of adequate supply ability in future times. Due to the addition of RESs like Solar energy, the LFC design has progressed into new strategies. This paper represents an impression of major issues regarding the addition of Solar Energy into frequency regulation power structure, which is most noticeable nowadays. MFO is a very talented and appealing algorithm due to its advantages like fast searching speed and simplicity but drawbacks like getting trapped in awful local optima due to exploitation-centered. Hence, it is important to take advanced algorithms like BMFO1, BMFO2, and HHO with a better concert to supplement the algorithm. This work presented a revised LFC model, which maintains the system frequency without any steady-state error, unlike conventional PI and Moth Flame Optimizer. It instantaneously responds to the different load disturbances and makes the system stable within a short time. The frequency reaction with the usage of RESs and related issues are examined, and the essential for revision of frequency performance standards is highlighted to be used in battery-operated hybrid vehicles.

Acknowledgement: The Authors acknowledge the support provided by the Deanship of Scientific Research (DSR) at King Abdulaziz University, Jeddah, Saudi Arabia for providing technical and financial support under Grant No. (FP-221-43). The Authors also acknowledge the support provided by King Abdullah City for Atomic and Renewable Energy (K.A.CARE) under K.A.CARE-King Abdulaziz University Collaboration Program.

Funding Statement: The Deanship of Scientific Research (DSR) at King Abdulaziz University, Jeddah, Saudi Arabia has funded this project, under grant no. (FP-221-43).

Conflicts of Interest: The authors declare that they have no conflicts of interest to report regarding the present study.

References

- [1] J. García, J. V. Martí and V. Yepes, "The buttressed walls problem: An application of a hybrid clustering particle swarm optimization algorithm," *Mathematics*, vol. 8, no. 862, pp. 1–22, 2020.
- [2] D. Prashar and K. Arora, "Design of two area load frequency control power system under unilateral contract with the help of conventional controller," *International Journal of Information Communication Technology and Digital Convergence*, vol. 5, no. 2, pp. 22–27, 2020.
- [3] E. O. I. and C. E. Fosha, "Optimum megawatt-frequency control of multiarea electric energy systems," *IEEE Transactions on Power Apparatus and Systems*, vol. 89, no. 4, pp. 556–563, 1970.
- [4] J. G. Ziegler and N. B. Nichols, "Optimum setting for automatic controllers," *Transactions of ASME*, vol. 64, no. 11, pp. 759–768, 1942.
- [5] S. Hossein, A. Heider and A. J. Shayanfar, "Multi stage fuzzy PID load frequency controller in a restructured power system," *Journal of Electrical Engineering*, vol. 58, no. 2, pp. 61–70, 2007.
- [6] S. Matlab, *MATLAB 9.4 version 9.4 (R2018a)*, MA: The MathWorks Inc., 2018.
- [7] B. S. Yildiz and A. R. Yildiz, "Moth-flame optimization algorithm to determine optimal machining parameters in manufacturing processes," *Materials Testing*, vol. 59, no. 5, pp. 425–429, 2017.
- [8] M. L. Kothari, B. L. Kaul and J. Nanda, "Automatic generation control of hydro-thermal system," *Journal of Institute of Engineers India*, vol. 61, no. 1980, pp. 85–91, 1980.

- [9] R. D. Christie and A. Bose, "Load frequency control issues in power system operations after deregulation," *IEEE Transactions on Power Systems*, vol. 11, no. 3, pp. 1191–1200, 1996.
- [10] C. T. Pan and C. M. Liaw, "An adaptive controller for power system load-frequency control," *IEEE Transactions on Power Systems*, vol. 4, no. 1, pp. 122–128, 1989.
- [11] S. Mirjalili, "Moth-flame optimization algorithm: A novel nature-inspired heuristic paradigm," *Knowledge-Based Syst*, vol. 89, no. 2015, pp. 228–249, 2015.
- [12] S. Reddy, L. K. Panwar, B. K. Panigrahi and R. Kumar, "Solution to unit commitment in power system operation planning using binary coded modified moth flame optimization algorithm (BMMFOA): Aflame selection based computational technique," *Journal of Computational Science*, vol. 25, no. 2018, pp. 298–317, 2018.
- [13] V. K. Kamboj, A. Nandi, A. Bhadoria and S. Sehgal, "An intensify harris hawks optimizer for numerical and engineering optimization problems," *Applied Soft Computing*, vol. 89, no. 2020, pp. 1–35, 2020.
- [14] N. Bekhouche and A. Feliachi, "Decentralized estimation for the automatic generation control problem in power systems," in *IEEE Conf. on Control Applications*, Dayton, OH, USA, pp. 621–632, 1992.
- [15] A. P. Birch, A. T. Sapeluk and C. S. Ozveren, "An enhanced neural network load frequency control technique," in *Int. Conf. on Control*, Coventry, UK, pp. 409–415, 1994.
- [16] O. I. Elgerd and H. H. Happ, "Electric energy systems theory an introduction," *IEEE Transactions on Systems, Man, and Cybernetics*, vol. 2, no. 2, pp. 296–297, 1972.
- [17] K. Arora, "Optimization methodologies and testing on standard benchmark functions of load frequency control for interconnected multi area power system in smart grids," *Mathematics*, vol. 8, no. 6, pp. 1–23, 2020.
- [18] H. Alhelou, "Challenges and opportunities of load frequency control in conventional, modern and future smart power systems: A comprehensive review," *Energies*, vol. 11, no. 10, pp. 1–35, 2018.
- [19] D. Xu, J. Liu, X. -G. Yan and W. Yan, "A novel adaptive neural network constrained control for a multi-area interconnected power system with hybrid energy storage," *IEEE Transactions on Industrial Electronics*, vol. 65, no. 8, pp. 6625–6634, 2017.
- [20] Y. Xu, C. Li, Z. Wang, N. Zhang and B. Peng, "Load frequency control of a novel renewable energy integrated micro-grid containing pumped hydropower energy storage," *IEEE Access*, vol. 6, no. 2018, pp. 29067–29077, 2018.